



**HAL**  
open science

## Material constitutive behavior identification at high strain rates using a direct-impact Hopkinson device

Xiaoli Guo, Cheikh-Tidiane Sow, Chady Khalil, Thomas Heuzé, Guillaume Racineux

► **To cite this version:**

Xiaoli Guo, Cheikh-Tidiane Sow, Chady Khalil, Thomas Heuzé, Guillaume Racineux. Material constitutive behavior identification at high strain rates using a direct-impact Hopkinson device. 7th International Conference on High Speed Forming (ICHSF), Apr 2016, Dortmund, Germany. hal-02279968

**HAL Id: hal-02279968**

**<https://hal.science/hal-02279968>**

Submitted on 5 Sep 2019

**HAL** is a multi-disciplinary open access archive for the deposit and dissemination of scientific research documents, whether they are published or not. The documents may come from teaching and research institutions in France or abroad, or from public or private research centers.

L'archive ouverte pluridisciplinaire **HAL**, est destinée au dépôt et à la diffusion de documents scientifiques de niveau recherche, publiés ou non, émanant des établissements d'enseignement et de recherche français ou étrangers, des laboratoires publics ou privés.



Distributed under a Creative Commons Attribution 4.0 International License

# Material constitutive behavior identification at high strain rates using a direct-impact Hopkinson device

X. Guo<sup>1</sup>, C. Sow<sup>1\*</sup>, C. Khalil<sup>1\*</sup>, T. Heuzé<sup>1</sup>, G. Racineux<sup>1</sup>

<sup>1</sup> Research Institute in Civil and Mechanical Engineering (GeM, UMR 6183 CNRS), École Centrale de Nantes (ECN), France

\*Corresponding authors. Email: cheikh-tidiane.sow@ec-nantes.fr, chady.khalil@ec-nantes.fr

## Abstract

*Modern numerical simulation techniques allow nowadays obtaining accurate solutions of magnetic pulse and electrohydraulic forming/welding processes. However, one major difficulty persists: the identification of material constitutive equations behavior at levels of high strain rates reached by these processes, and which varies between  $10^3$  and  $10^5$   $s^{-1}$ .*

*To address this challenge, a direct-impact Hopkinson system was developed at ECN. It permits to perform dynamic tests at very high strain rates exceeding the range of the traditional Split Hopkinson Pressure Bars and hence enable us to identify constitutive models for a wide range of strain rates. The alloy used to test this device was Ti-6Al-4V.*

*Strain rates up to  $2.5 \times 10^3$   $s^{-1}$  were attained.*

## Keywords

Direct impact Kolsky bar, inverse analysis, high strain rate, elastic-viscoplastic, constitutive models

## 1 Introduction

To further develop electromagnetic or electrohydraulic forming, crimping or welding processes, accurate simulation of these processes is needed. This goes by the study of the material performance at high strain rates and to define a precise dynamic behavior by using constitutive models. The strain rates involved can be up to  $10^5$   $s^{-1}$ . It is well known that the behavior of many metallic materials usually depends on the strain rate; therefore, a

good representation of this behavior is required by the mean of dynamic tests on a wide range of strain rates. The most popular experiment is the classical Split Hopkinson Pressure Bar (SHPB) (Davies 1948; Kolsky 1949) capable to attain strain rates ranging up to  $10^4 \text{ s}^{-1}$  (Gorham et al. 1992; Ramesh 2008). For higher strain rates, another system of the SHPB is available: a direct-impact Hopkinson device (Dharan & Hauser 1970). In this device, the incident bar is removed and very high strain rates of the order of  $10^5 \text{ s}^{-1}$  can be achieved (Dharan & Hauser 1970; Kamler et al. 1995). In the present work, the Ti-6Al-4V alloy is tested at strain rates varying from 3000 to 25000  $\text{s}^{-1}$  using a direct-impact Hopkinson device and an elastic-viscoplastic constitutive model is identified by using an inverse identification.

## 2 Direct-impact tests on the Ti-6Al-4V at very high strain rate

This device is composed of a transmitted bar, a projectile and three Wheatstone bridges of double gauges mounted on the bar for the measurement of deformations and dispersion monitoring (**Figure 1**). The transmitted bar is 1.2m length and 10 mm diameter. Four projectiles of diameter 15.8 mm and lengths of 500 mm, 125 mm, 60 mm and 30 mm respectively are used.

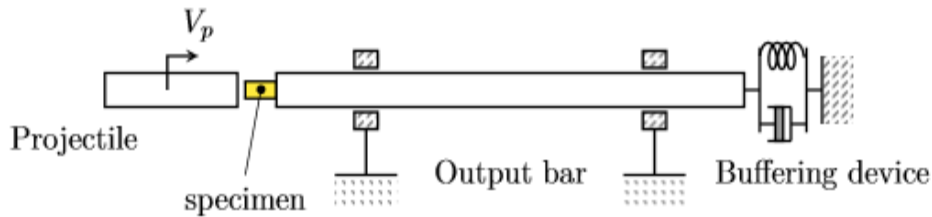


**Figure 1:** direct impact device

The higher the objective strain rate is, the lower the length of the projectile must be to avoid crushing the specimen. The bar and the projectiles are made of MARVAL X2NiCoMo18-8-5, with a yield stress of 1800 MPa. The impact velocity of the projectile is measured by two laser diodes. For each objective strain rate, the value of the specimen length  $l_s$ , the projectile length  $l_p$  and its impact velocity  $v_p$  should be determined. The maximum values of the expected strain rate  $\dot{\epsilon}_s$  and the allowable strain  $\epsilon_s$  in the specimen can be approximated by the following equation:

$$\dot{\epsilon}_{smax} \approx \frac{v_p}{l_s} \quad \epsilon_{smax} \approx \frac{\dot{\epsilon}_s 2l_p}{c_p} \quad (1)$$

where  $c_p$  denotes the sound speed in the projectile.  $c_p$  is defined by the equation  $\sqrt{E/\rho}$ .  $E$  and  $\rho$  are respectively the Young's modulus and the density of the projectile material. The parameters for each objective strain rate (Obj.  $\dot{\epsilon}_s$ ) are listed in Table 1.

Test n°	Obj. $\dot{\epsilon}_s$ (s <sup>-1</sup> )	$v_p$ (m/s)	$l_p$ (mm)	$l_s$ (mm)	$\dot{\epsilon}_{smax}$ (s <sup>-1</sup> )	$\epsilon_{smax}$	Test n°	Obj. $\dot{\epsilon}_s$ (s <sup>-1</sup> )	$v_p$ (m/s)	$l_p$ (mm)	$l_s$ (mm)	$\dot{\epsilon}_{smax}$ (s <sup>-1</sup> )	$\epsilon_{smax}$
T1	3000	15	500	5	3064	0.11	T7	18000	36	60	2	17970	0.33
T2	5000	25	125	5	4612	0.16	T8	18000	30	60	1.5	18350	0.16
T3	7000	28	125	4	6925	0.17	T9	20000	30	60	1.5	21222	0.23
T4	10000	30	60	3	10740	0.17	T10	20000	40	30	2	19659	0.24
T5	12000	36	60	3	12040	0.25	T11	25000	37.5	30	1.5	25050	0.25
T6	15000	30	60	2	15010	0.11							

**Table 1:** experimental plan and results

The elastic strain  $\epsilon_b(t)$  in the transmitted bar and the impact velocity  $v_p$  of the projectile are measured. From the recorded strain  $\epsilon_b(t)$ , the force  $F_s(t)$  applied by the projectile on the specimen is computed by:

$$F_s(t) = E_b S_b \epsilon_b(t) \quad (2)$$

where  $E_b$  is the Young's modulus and  $S_b$  is the cross-section of the bar. The results are plotted in Figure 2. The trays observed during the unloading part of these curves arise from the shorter length of the projectile than that of the bar and the mismatch of the generalized wave impedances between the projectile  $Z_p = (\rho c S)_p$ , the specimen  $Z_s = (\rho c S)_s$  and the bar  $Z_b = (\rho c S)_b$  (Wang 2007).

When the projectile is long enough, the loading time and the characteristic time are equivalents, as we can see in the Figure 2(a) where the projectile is 500 mm length. As the projectile shorten the actual period of loading of the specimen lasts approximately twice the characteristic time or even longer as is observed in Figure 2(b) and Figure 2(d), these results from the different cross-sections of the projectile and the bar. Following this, the specimen undergoes a second compression before the unloading starts. Thus, it is subjected to a higher strain than that of the test T1 as shown in the Table 1, even though the projectile of the test T1 has a greater kinetic energy before impact.

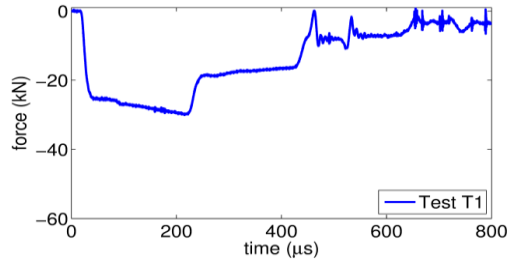
For the direct impact device, the strain rate in the specimen is assessed by the following equation (Gorham et al. 1992; Guo et al. 2014):

$$\dot{\epsilon}_s(t) = - \frac{v_p + \frac{S_p + S_b}{S_p} C_b \epsilon_b(t)}{l_s} \quad (3)$$

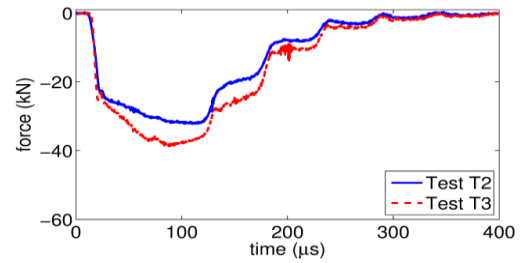
where  $S_p$  is the cross-section of the projectile and  $C_b$  the sound speed of the bar. The maximum compressive strain rate  $\dot{\epsilon}_{smax}$  computed by using this equation and the measured compressive strain  $\epsilon_{smax}$  for each test are listed in Table 1. This equation states that the compressive strain rate gets its maximum equal to  $v_p/l_s$  at the beginning of the impact and is however only valid during the characteristic time (Gorham et al. 1992).

The stress-strain curves are computed using the classical analysis of the Hopkinson tests (Guo 2015). The results are shown in the Figure 3. As the strain rate increases, the curves exhibit a rising strain hardening. However, they are subjected to scattering, as we can observe through small oscillations. Consequently, the rate dependency is difficult to be

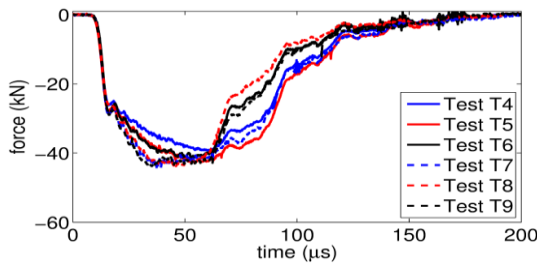
assessed on these curves directly. An inverse analysis is carried out for the identification of the constitutive models.



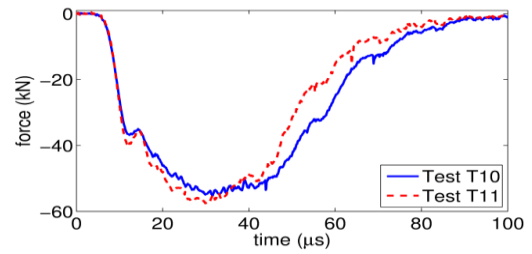
(a) Projectile length 500 mm



(b) Projectile length 125 mm

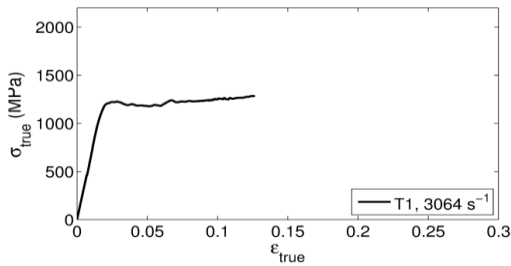


(c) Projectile length 60 mm

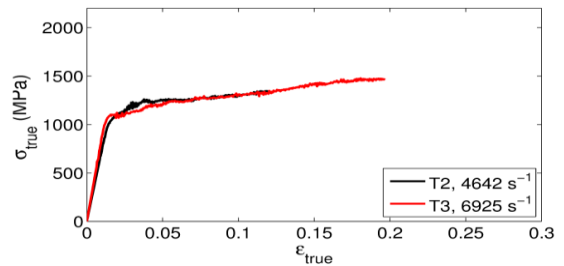


(d) Projectile length 30 mm

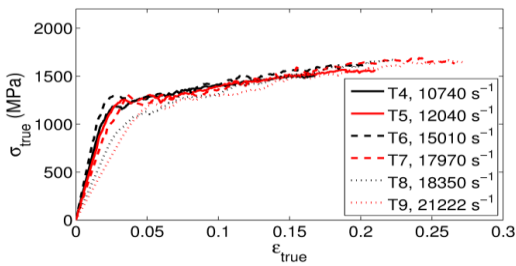
**Figure 2:** Force on specimen in the direct impact tests



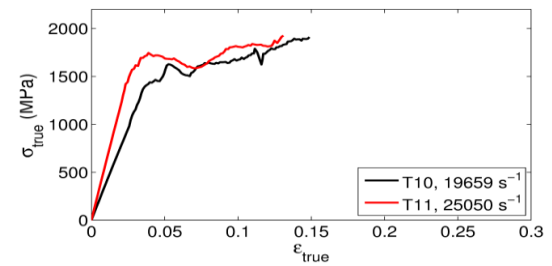
(a) Projectile length 500 mm



(b) Projectile length 125 mm



(c) Projectile length 60 mm



(d) Projectile length 30 mm

**Figure 3:** Stress-strain curves of the Ti-6Al-4V

### 3 Inverse identification of elastic-viscoplastic constitutive models

The elastic-viscoplastic constitutive models used to represent the behavior of the material must be able to fit correctly the experimental measurements. They are identified by an inverse procedure that uses a dynamic numerical analysis. No thermal effect is addressed in these identifications. Three models that fit well to this requirement have been chosen:

- a) The Johnson-Cook model (Johnson & Cook 1983)

$$\sigma(p, \dot{p}) = (A + Bp^n)(1 + C \ln \frac{\dot{p}}{\dot{p}_0}) \quad (4)$$

where  $p$  and  $\dot{p}$  are the cumulated plastic strain and strain rate respectively. The parameters  $A$ ,  $B$  and  $n$  are obtained by quasi-static classical tension test [10]:  $A=955$  MPa,  $B=770$  MPa and  $n=0.557$ . The parameter  $C$  is the only one to be identified by the inverse process. An axisymmetric 2D Finite Element model in ABAQUS is used to compute the dynamic simulation. The model consists of the projectile, the specimen and the bar.

- b) The Zerilli-Armstrong model (Zerilli & Armstrong 1996)

This model is calibrated using a unidimensional FE model in MATLAB developed in (Andriamiseza 2014). Assuming a constant temperature  $T$ , two variants for bcc and hcp materials are considered in Eq. 5 and Eq. 6 respectively:

$$\sigma_y = K_0 + K_1 p^n + K_2 \dot{p}^{K_3} \quad (5)$$

where  $K_0 = C_0$ ,  $K_1 = C_5$ ,  $K_2 = C_1 \exp(-C_3 T)$  and  $K_3 = C_4 T$ . The parameters,  $K_0$ ,  $K_1$  and  $n$  have the same value as the parameters  $A$ ,  $B$  and  $n$  of the Johnson-Cook relation because of the equivalent form of strain hardening. The parameters  $K_2$  and  $K_3$  have been calibrated inversely.

$$\sigma_y = K_0 + K_1 \dot{p}^{K_2} + K_3 \sqrt{p \dot{p}}^{K_4} \text{ (hcp)} \quad (6)$$

where  $K_0 = C_0$ ,  $K_1 = C_1 \exp(-C_3 T)$ ,  $K_2 = C_4 T$ ,  $K_3 = C_2 \exp(-C'_3 T)$  and  $K_4 = C'_4 T$ .  $K_0$  is equivalent to the yield stress. Four parameters  $K_1$ ,  $K_2$ ,  $K_3$  and  $K_4$  are computed during the inverse identification.

The cost function  $f(x)$  is defined as the Euclidean norm of the difference between the simulated strain  $\varepsilon_{sim}(x, t)$  and the recorded strain  $\varepsilon_{exp}(t)$ . The identification is done on each tests of the Table 1. The calibrated strain  $\varepsilon_{sim}$  of the tests T1, T4, T6, T8 and T11 are plotted and superposed to the measured strain  $\varepsilon_{exp}$  in the Figure 4(a)-

Figure 4(e). An error bar is plotted associated to each mean value of the parameter  $C$  for the 2D identification, as shown in the

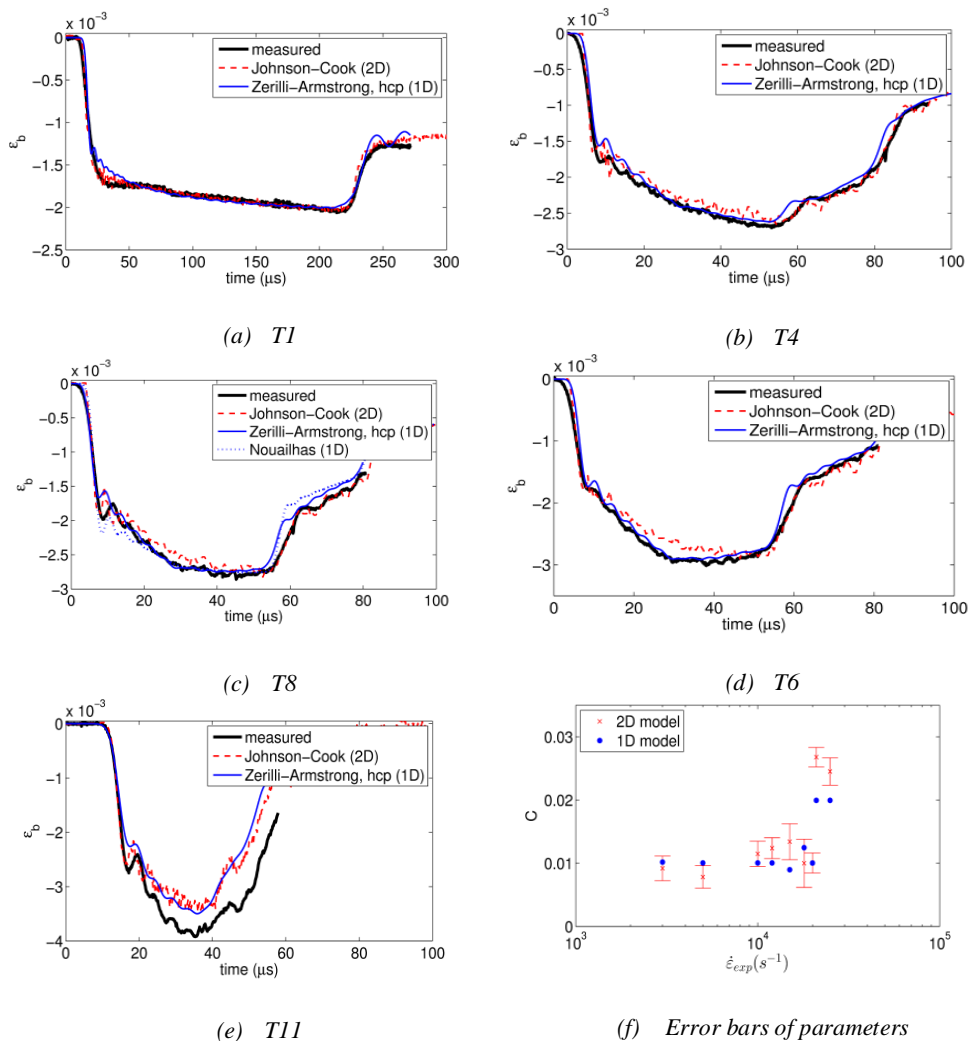
Figure 4(f). At least two repetitions are carried out for each test. The simulated strains of the three different constitutive models fit well to the experimental data at strain rate up to  $15000\text{ s}^{-1}$ . We observe at the second raising stage when the specimen is plastically deformed that the results are concordant as shown in the

Figure 4(a)-

Figure 4(c). A small difference appears at this stage between the calibrated strain of the Johnson-Cook model and the measured one in the

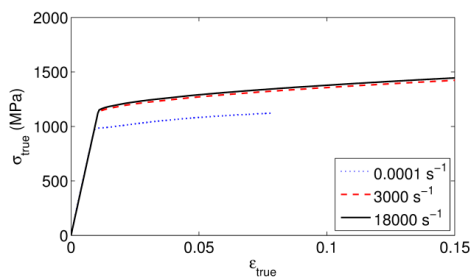
Figure 4(d). The Zerilli-Armstrong model fits well the experimental data. The

Figure 4(f) indicates that an approximately constant value of the parameter  $C$  of the Johnson-Cook model is identified at the strain rate ranging from  $3000$  to  $18000\text{ s}^{-1}$ . At very high strain rate as observed in the tests T10 and T11, a much greater value of  $C$  is obtained. The differences in these two tests may be due to (i) the very short projectile used in the test and/or (ii) the thermal effects not addressed in the identification. More repetitions of these tests must be carried out to clarify the results.

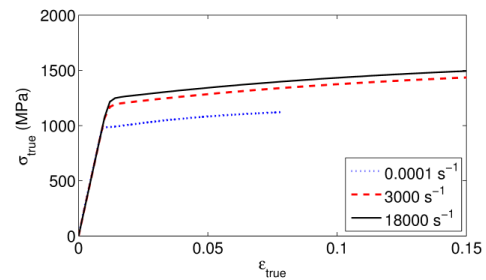


**Figure 4: Results of identifications**

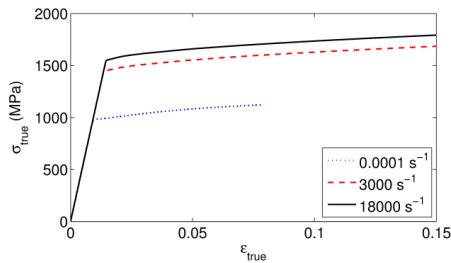
The stress-strain curves of the identified constitutive models are plotted at the strain rate of  $3000\text{ s}^{-1}$  and  $18000\text{ s}^{-1}$  and are compared to those obtained from the quasi-static tests in the Figure 5. The Figure 5(a)-Figure 5(c) show a great raise of the flow stress as the strain rate is increased. This increase is lower when the strain rate goes from  $3000$  to  $18000\text{ s}^{-1}$ . For the Johnson-Cook model, the two curves at these two strain rates are very close in the Figure 5(a). Similar observations can be done for the other models.



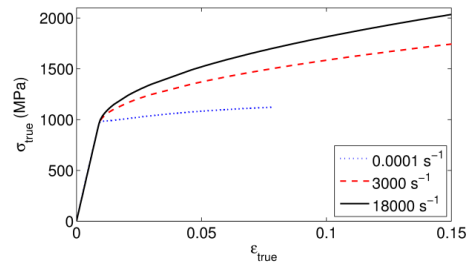
(a) Johnson-Cook model



(b) Nouaillhas model



(c) Zerilli-Armstrong (bcc)



(d) Zerilli-Armstrong (hcp)

**Figure 5: stress-strain curves plotted within the range of  $10^{-4}$  to  $18000\text{ s}^{-1}$** **4 Conclusion**

In this work, the Ti-6Al-4V has been tested on a range of strain rate ranging from  $3000$  to  $25000\text{ s}^{-1}$  using the direct-impact Hopkinson device. To identify three elastic-viscoplastic constitutive models, an inverse analysis has been carried out on the experimental data. The three identified constitutive models fit well the experimental data at the strain rate ranging from  $3000$  up to  $18000\text{ s}^{-1}$ . However more experimental and numerical research at higher strain rate is required to refine these results.



## References

- Andriamiseza, A., 2014. *Rapport de stage de Master: Identification de modèles de comportement à haute vitesse de déformation sur des essais de Kolsky à impact direct*,
- Davies, R.M., 1948. A critical study of the Hopkinson Pressure Bar. *Philosophical Transactions of the Royal Society of London. Series A. Mathematical and Physical Sciences*, 240(821), pp.375–457.
- Dharan, C.K.H. & Hauser, F.E., 1970. Determination of stress-Strain characteristics at very high strain rates. *Experimental Mechanics*, 10(9), pp.370–376.
- Gorham, D.A., Pope, P.H. & Field, J.E., 1992. An improved method for compressive stress-strain measurements at very high strain rates. *Philosophical Transactions of the Royal Society of London. Series A. Mathematical and Physical Sciences*, 438(1992), pp.153–170.
- Guo, X. et al., 2014. Inverse identification at very high strain rate of the Johnson--Cook constitutive model on the Ti-6Al-4V alloy with a specially designed direct-impact Kolsky bar device. *Strain*, 50(6), pp.527–538.
- Guo, X., 2015. *On the direct impact Hopkinson system for dynamic tests at very high strain rates*. Ecole centrale de Nantes.
- Johnson, G.R. & Cook, W.H., 1983. A constitutive model and data for metals subjected to large strains, high strain rates and high temperatures. *7th International Symposium on Ballistics*, pp.541–547.
- Kamler, F., Niessen, P. & Pick, R.J., 1995. Measurement of the behaviour of high-purity copper at very high rates of strain. *Canadian Journal of Physics*, 73(5--6), pp.295–303.
- Kolsky, H., 1949. An investigation of the mechanical properties of materials at very high rates of loading. *Proceedings of the Physical Society. Section B*, 62.
- Ramesh, K.T., 2008. Part D: Chapter 33. High strain rate and impact experiments. In *Springer handbook of experimental solid mechanics*. Springer, pp. 1–31.
- Wang, L., 2007. *Foundations of stress waves*, Elsevier BV.
- Zerilli, F.J. & Armstrong, R.W., 1996. Constitutive relations for titanium and Ti-6Al-4V. In *Proceedings of the conference of the American Physical Society topical group on shock compression of condensed matter*. pp. 315–318.